# The OSCAR code: modelling and simulation of the corrosion product behaviour under nucleate boiling conditions in PWRs

Alexandre Ferrer, Frédéric Dacquait, B. J. P. Gall, Gilles Ranchoux, Mathieu Corbineau

10142

# The OSCAR code: modelling and simulation of the corrosion product behaviour under nucleate boiling conditions in PWRs

Alexandre FERRER[1], Frédéric DACQUAIT[2], Benoit GALL[3], Gilles RANCHOUX[4], Mathieu CORBINEAU [5]

1: ex-CEA, DEN, France
2: CEA, DEN, France
3: IPHC/UDS, France
4: EDF/SEPTEN, France
5: Areva NP, France

## ABSTRACT

The PWR primary circuit materials are subject to general corrosion leading to metallic elements (mainly Fe, Ni, Cr, Mn, Co) transfer and subsequent ion precipitation and particle deposition processes on the primary circuit surfaces. When deposited on fuel rods, these species are activated by neutron flux. Thus, crud erosion and dissolution processes result in primary coolant activities.
During a normal operating cycle in an EDF PWR, the volume activities in the coolant are relatively stable (usually about 10-30 Bq.g-1 in 58Co). During some cycles (depending on fuel management), a significant increase in 58Co and 51Cr volume activities can be observed (10 to 100 times the ordinary volume activities). This increase in volume activities is due to local sub-cooled nucleate boiling on the hottest parts of some fuel assemblies. Indeed, it is well known that nucleate boiling enhances the deposition and precipitation processes.

Crud growth in boiling conditions is related to different phenomena:

- Enrichment: concentration increases at crud-coolant interface,
- Boiling deposition by vaporisation: fluid vaporization at wall results in particle deposition and ion precipitation. As the crud growth, boiling occurs in the crud itself, so do the ion precipitation and deposition of the small particles.
- Boiling deposition by trapping: some of the small particles trapped at the interface bubble/fluid make deposit when a bubble leaves the wall.
- Enhanced erosion: turbulences generated by bubbles collapsing close to the wall and spalling above a certain deposit thickness enhance erosion; it results in the release of particle agglomerates.

These phenomena have been modelled in the OSCAR V1.3 code.

In this article, we present the modelling of these mass transfer mechanisms in boiling conditions and we show that the crud amount on fuel rods and the volume activities in the primary coolant in case of boiling calculated by OSCAR are in accordance with the experimental feedback on French PWRs.

**Keywords:** Corrosion products, nucleate boiling, PWR, OSCAR

# 1 INTRODUCTION

The PWR primary circuit materials are subject to general corrosion leading to metallic elements (mainly Fe, Ni, Cr, Mn, Co) transfer and subsequent ion precipitation and particle deposition processes on the primary circuit surfaces. When deposited on fuel rods, these species are activated by neutron flux. Thus, crud erosion and dissolution processes result in primary coolant activities.

During a normal operating cycle in an EDF PWR, the volume activities in the coolant are relatively stable (usually about 10-30 $Bq.g^{-1}$ in $^{58}Co$). During some operating cycles (depending on fuel management), a significant increase in $^{58}Co$ and $^{51}Cr$ volume activities can be observed (10 to 100 times the ordinary volume activities) generally in the second half of the cycle (see Figure 1). The PWR operation feedback shows that the volume activities in these cases are mainly due to particles, indicating that these increases in volume activities are due to erosion of thick crud on fuel rods. This thick crud is due to local sub-cooled nucleate boiling on the hottest parts of some fuel assemblies. Indeed, it is well known that nucleate boiling enhances the deposition and precipitation processes. The thickness of the crud layer can reach 100 µm in boiling areas and it is sometimes linked to CIPS (Crud Induced Power Shift) in extreme cases [1].

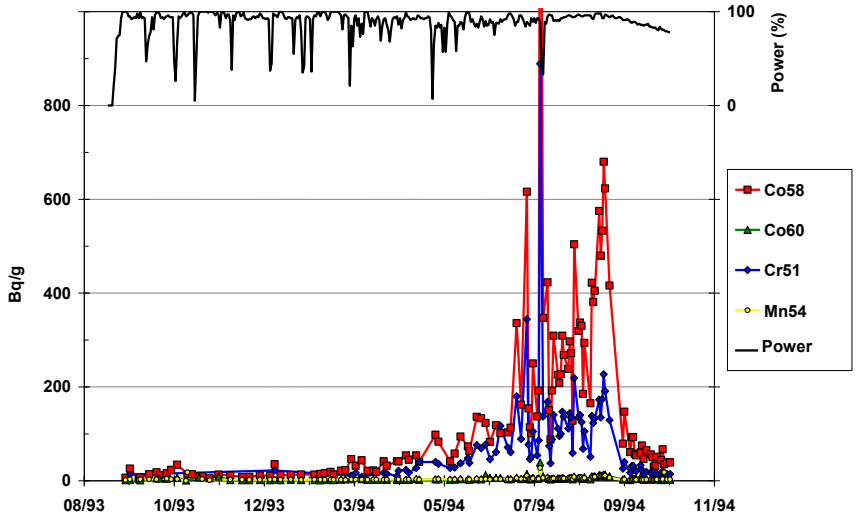


**Figure 1. $^{58}Co$, $^{60}Co$, $^{51}Cr$ and $^{54}Mn$ volume activities during an operating cycle with increase in $^{58}Co$ and $^{51}Cr$**

The modelling of the crud growth and erosion fluxes in cases of non-boiling and boiling flows are essential to enable calculations of surface masses and volume activities in the coolant. In partnership with EDF and Areva NP, the CEA has developed the OSCAR calculation code to predict the surface and volume activities in the PWR primary circuit and the amount of deposited/precipitated material on the primary circuit surfaces [2]. One further improvement of this calculation code is the simulation of the deposited/precipitated/eroded material due to nucleate boiling. This development was the subject of a PhD thesis [3] and is presented in this paper.

In a first part we will present the phenomenology of the crud growth, then the mass transfer mechanisms in nucleate boiling conditions developed for the OSCAR code and finally the crud amount on fuel rods and the volume activities in the primary coolant in case of boiling calculated by OSCAR and their comparison to the experimental feedback on French PWRs.

## 2 PHENOMENOLOGY OF CRUD GROWTH

In a region with sub-cooled nucleate boiling, the crud can be described as a porous media. The void proportion in the magnetite crud was measured to be about 60% to 70% according to Macbeth [4] and Jones [5]. The pore size is of the order of the particle size in the coolant with a typical pore diameter size between 0.1 and 0.5 µm. Furthermore, the formation of a very regular distribution of large pore holes (diameter of about 5 µm) penetrating deep into the deposit is observed (these are called chimneys) [4].
In the case of local nucleate boiling, two cases may arise:

- the coolant/crud interface (wall) temperature $T_w$ is equal to the wall boiling temperature $T_b$ (Case 1),
- the coolant/crud interface temperature is lower than the wall boiling temperature, critical temperature for boiling may only occur inside the crud above a given thickness (Case 2).

In Case 1, boiling occurs directly at the wall. As illustrated in Figure 2, in the case of local nucleate boiling at the surface, phenomenology of crud growth can be divided into three mains steps:

- Boiling starts at the crud/fluid interface as soon as boiling temperature is reached. It is worth pointing that boiling process needs an overheat ($\Delta T_{sat}$), boiling temperature being $T_b = T_{sat} + \Delta T_{sat}$ (Figure 2.a).
- Crud is formed on fuel rod clad due to particle deposition and ion precipitation, which are enhanced by boiling. Since crud is a high porosity medium, boiling can start with a lower boiling temperature than in the case of a heated flat surface in contact with the fluid. So, as the crud grows, boiling process is not located anymore at the coolant/crud interface but in the crud itself (Figure 2.b).
- To run this process, porosity feeds the boiling with fluid thanks to capillarity pumping action [4, 6]. This operating mode generates chimneys through action of the steam exhaust and feeds surrounding crud (Figure 2.c). This induces progressive filling of the porosity with ions and particles as well as crud thickness increases.

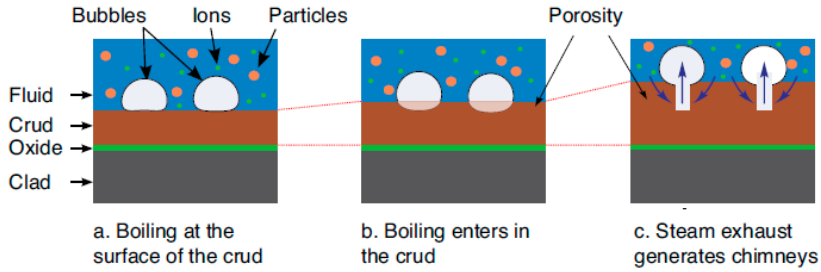


**Figure 2. Illustration of crud growing process in Case 1. Wall temperature is above the wall boiling temperature ($T_w = T_b$)**

In Case 2, where the wall temperature is slightly lower than the boiling temperature, the process also implies three phases illustrated in Figure 3:

- The crud grows in a first phase by particle deposition and ion precipitation in single-phase flow (see Figure 3.a). The oxide/crud interface temperature increases as the crud grows (effect of the crud thermal resistivity).
- When oxide/crud interface reaches the boiling temperature, bubbles are created by boiling action inside the crud (see Figure 3.b). Boiling is fed by coolant fluid pumped through capillarities. This fluid motion generates porosity filling inside the crud as well as crud extension at crud/fluid surface (so porosity decreases in the crud).
- This process can go up the generation of a superheated vapour layer at the oxide/crud interface. Thanks to crud inhomogeneities, some steam exit paths may be favoured, inducing chimneys creation in further crud grow process as it is the case in Case 1 (see Figure 3.c).

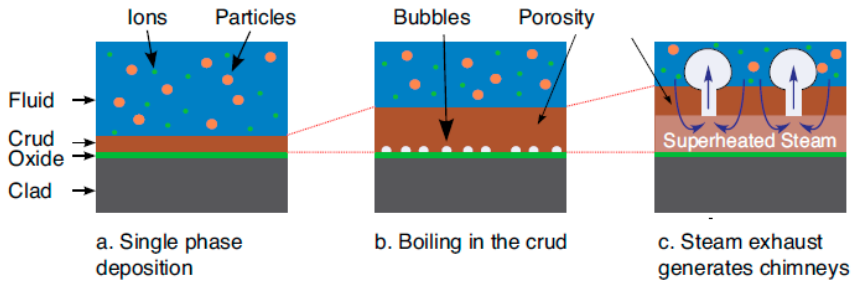


**Figure 3. Illustration of crud growing process in Case 2. Wall temperature is below the wall boiling temperature ($T_w < T_{b)}$**

# 3 MODELLING OF MASS TRANSFER MECHANISMS IN BOILING CONDITIONS

## 3.1 Enrichment phenomenon

Boiling action at the wall or in the crud implies an imbalance between ion and particle radial advection flows from the coolant to the wall region and from the wall region to the coolant. Thus, ion and particle concentrations near the wall are higher than the ones in single-phase flow [7]. This phenomenon is called “enrichment”. The ratio of the wall concentration $C_{wall}$ to the coolant concentration without boiling $C_0$ is called “enrichment factor” $F_E$, for a considered species:

$$F_E = \frac{C_{wall}}{C_0} \quad (1)$$

The enrichment factor can be moderated if particles and ions are absorbed by the capillarity action to feed boiling in case of boiling in the crud.

### 3.1.1 Enrichment factor - Boiling at the wall (Case 1)

In order to give a realistic description of the enrichment factor when nucleate boiling occurs directly at the wall, we consider the fluid as three layers radially organized around fuel rod (See Figure 4) [7]:

- The first layer, called Zone L, is the laminar layer. We assume that the ion and particle concentrations ($C_{wall}$) are constant in this region.
- The second layer, called Zone P, composes the intermediate zone. In this intermediate layer, turbulences tend to homogenize the fluid temperature and species concentrations. The thickness of this fluid layer is assumed to be equal to the detachment radius of bubbles, namely a few tens of micrometers.
- The last layer, called Zone C, is fully turbulent. The average void fraction is considered to be less than 2% in this zone.

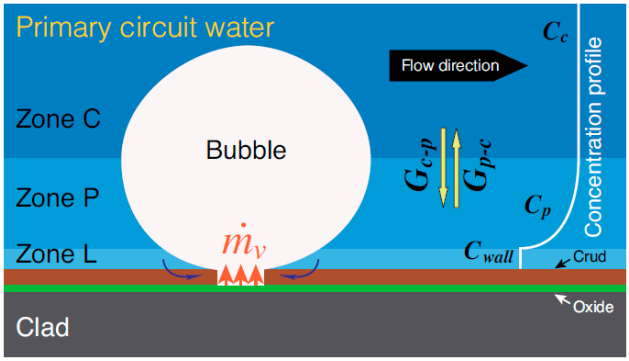


**Figure 4. Illustration of the three fluid regions model in Case 1**

In order to estimate the enrichment factor, a mass balance is done at the wall vicinity based on this three-layer structure and on the assumption that the superheated fluid layer thickness is thin enough to neglect recondensation effect. The thickness of this superheated layer is supposed to be equal to the bubble radius at detachment.
By a mass balance in Zone P and Zone L and assuming that:

$$C_p = k \cdot C_{wall} + (1 - k) \cdot C_c \quad \textbf{(2)}$$

with k a constant depending on the thicknesses of Zone P and Zone L, March [7] obtained:

$$\frac{C_C}{C_0} = \frac{1}{(1-x)+\Gamma \cdot x} \quad \textbf{(3)}$$

and

$$F_E = \frac{C_{wall}}{C_C} \cdot \frac{C_C}{C_0} = \frac{n_c + (1/k)\cdot(1-\Gamma) - 1}{n_c - 1} \cdot \frac{1}{(1-x)+\Gamma \cdot x} \quad \textbf{(4)}$$

with $n_c$ the circulation number ($n_c = G_{c-p}/\dot{m}_v$ with $G_{c-p}$ the fluid radial flow rate from Zone C to Zone P and $\dot{m}_v$ the vaporisation rate), x the mass quality and $\Gamma$ the volatility of a considerate species.

### 3.1.2 Enrichment factor - Boiling in the crud (Case 2)

The enrichment factor of equation (4) is only valid in the case of boiling at the wall. When boiling occurs in the crud, particles and ions are trapped due to capillarity action. The corrosion products concentration is very close to the equilibrium concentration and they are not volatile. So, we can consider that each particle or ion driven by the capillary forces is trapped in or on the crud (deposition/precipitation). A flow balance in the crud shows that the pumped liquid flow rate $G_{pump}$ in the crud is equal to the vaporization rate $\dot{m}_v$ corresponding to the liquid mass vaporized and driven to the bubbles nucleation sites:

$$\mathbf{G_{pump}} = \dot{m}_v \quad \textbf{(5)}$$

Considering the pumping action, we have:

$$\mathbf{G_{c-p} = G_{p-c} +} \dot{m}_v \quad \textbf{(6)}$$

$$\mathbf{G_{c-p} \cdot C_c = G_{p-c} \cdot C_p + G_{pump} \cdot C_{wall}} \quad \textbf{(7)}$$

By combining equations (2), (3), (5), (6) and (7), we obtain $C_{wall}/C_C = 1$ and then the enrichment factor in Case 2 is equal to:

$$F_E = \frac{1}{(1-x)+\Gamma \cdot x} \quad \textbf{(8)}$$

For corrosion products under PWR conditions, the mass quality and the volatility being almost 0, the enrichment factor in Case 2 is practically equal to 1.

Between the extreme values of the enrichment factor of Case 1 and Case 2, we have defined a linear interpolation as a function of the thicknesses of the crud and the fluid layer under a bubble [3]. The enrichment factor decreases with the crud growth due to the pumping effect (see an illustration in Figure 5).

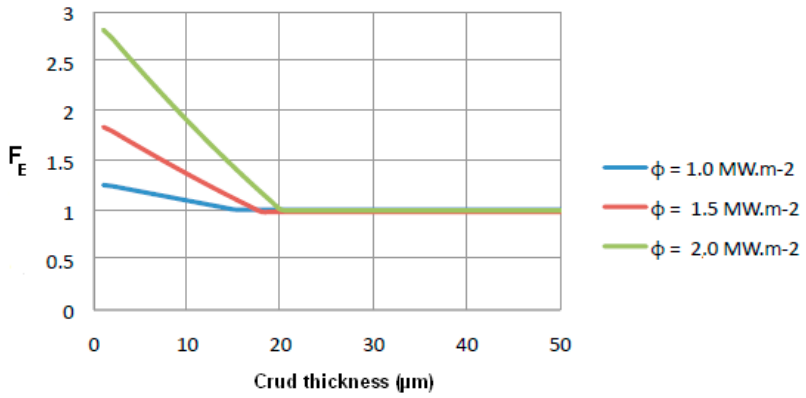


**Figure 5. Enrichment factor as a function of the crud thickness for different values of heat flux density Φ (P = 155 bar, G = 3500 kg·m$^{-2}$·s$^{-1}$)**

### 3.1.3 Enrichment - Precipitation/Dissolution at the wall

The mechanisms of precipitation and dissolution at the wall of the OSCAR code [2] are modified to take into account the enrichment at the wall.
The expression of the precipitation rate [kg.m$^{-2}$.s$^{-1}$] becomes:

$$\frac{dm}{dt} = h \cdot (F_E \cdot C_0 - C^{equil}) \quad \textbf{(9)}$$

and the dissolution rate:

$$\frac{dm}{dt} = \frac{1}{1/h + 1/V_{dissol}} \cdot (C^{equil} - F_E \cdot C_0) \quad \textbf{(10)}$$

with h the mass transfer coefficient of ions in the fluid [m.s$^{-1}$], $V_{dissol}$ the dissolution velocity coefficient (dissolution surface reaction rate coefficient) [m.s$^{-1}$], $F_E$ the enrichment factor, $C_0$ the bulk concentration of an element [kg.m$^{-3}$] and $C^{equil}$ the equilibrium concentration of the element [kg.m$^{-3}$] calculated by the OSCAR chemistry module, PhreeqCEA [8].

## 3.2 Boiling deposition

### 3.2.1 Boiling deposition by vaporization

Particles contained in the fluid sub-layer vaporized during the growth of a bubble are deposited on the wall. As well, non volatile ions contained in this fluid sub-layer precipitate directly on the wall or precipitate on particle contained in the sub-layer and then are deposited. Thus, note that the term “deposition by vaporization” also refers to precipitation by vaporization.
We propose to use the following mechanism for the boiling deposition by vaporization. This mechanism is based on Asakura studies [9]. The boiling deposition rate by vaporization [kg.m$^{-2}$.s$^{-1}$] is expressed by:

$$\frac{dm}{dt} = K_{vap} \cdot \dot{m}_v \cdot F_E \cdot C_0 \quad \textbf{(11)}$$

with $K_{vap}$ a constant (see below), $\dot{m}_v$ the vaporization rate [kg.m$^{-2}$.s$^{-1}$], $F_E$ the enrichment factor and $C_0$ the ion/particle concentration in the bulk [kg.kg$^{-1}$].
The main differences with the Asakura expression are:

- Use of the vaporization rate $\dot{m}_v$ instead of the maximum vaporization rate $\Phi/L$ (L: latent heat of vaporization). Indeed, in the Asakura experiment, the flow at the end of

the test section is in vapour form. In our case, the void fraction at the end of the core is about 1% to 2%;

- For a given species, use of the wall concentration $C_{wall} = F_E \cdot C_0$ (higher ion/particle concentration in a boiling region close to the wall due to boiling) instead of the bulk concentration;
- Extension to ionic species, ions contained in the micro-layer precipitate due to the increase of the concentration by vaporization of this fluid micro-layer.

### 3.2.1.1 Calculation of $K_{vap}$ - Boiling at the crud/fluid interface

According to Asakura, the $K_{vap}$ constant is the ratio of the volume used to form the dry region ($V_2$) to the total volume used to form a bubble during step 2 to step 3 ($V_1$). These volumes are schematized in Figure 6. The $K_{vap}$ constant calculated by geometric relations is equal to [3]:

$$K_{vap} = \frac{V_2}{V_1} = \frac{1}{2} \cdot \left(\frac{4}{3}\right)^3 \cdot \frac{R_b}{\delta_b} \cdot \left(\frac{\rho_v}{\rho_l}\right)^2 \qquad \textbf{(12)}$$

with $R_b$ the maximum bubble radius (radius at detachment) calculated by the Unal model [10], $\delta_b$ the maximum micro-layer thickness calculated by the Torigai model [11], $\rho_v$ and $\rho_l$ respectively the density of vapour and liquid.

Note that the expression of the $K_{vap}$ constant calculated here is different than the Asakura one by a factor 1/2.

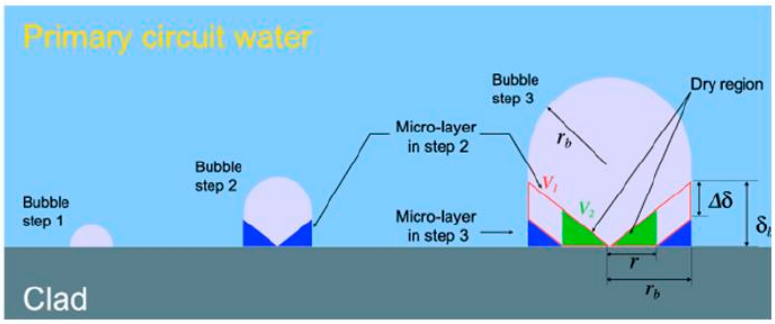


**Figure 6. Bubble growth on a heated surface**

Figure 7 presents the variation of the $K_{vap}$ constant with pressure, experimental data are reported. The expression considered in our study (blue curve) fits very well with the values of Charlesworth [12] (one of the two values), Rassokhim [13] and Turner [14].

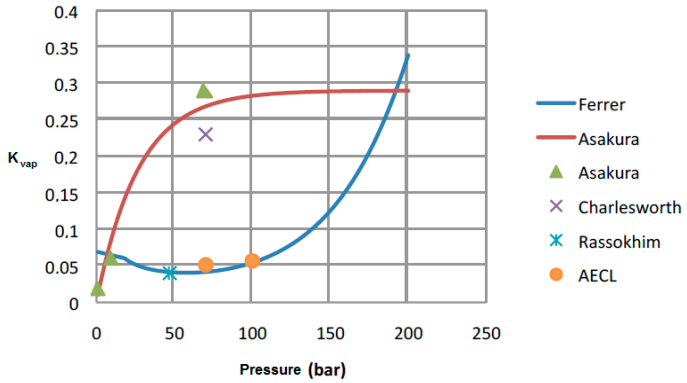


**Figure 7. Variation of $K_{vap}$ with pressure**

#### 3.2.1.2 Calculation of $K_{vap}$ - Boiling in the crud

The Asakura expression of the deposition rate is only valid in the case of boiling at the crud/fluid interface. However, in the case where boiling occurs deeper in the crud, if we suppose that bubbles are formed with the same volume $V_1$ between step 2 and step 3, all particles contained in this volume are trapped in the deposit by the capillary action. In this limit case, the particles and ions contained in the volume $V_1$ are deposited or precipitated, thus the $K_{vap}$ constant is equal to 1.

The $K_{vap}$ constant increases as the crud grows. We propose to use a linear variation as a function of the maximum micro-layer thickness and the crud thickness from the value of $K_{vap}$ calculated at the wall (eq. 12) and the value of 1 [3].

### 3.2.2 Boiling deposition by trapping

Basset *et al.* [15] and Thomas *et al.* [16] observed another kind of deposit (in sub-cooled boiling regions), deposit in form of ring, different than the one formed by micro-layer vaporization studied by Asakura (deposit in form of spot). They explained the ring formation by the fact that small particles (i.e. colloids) are trapped at the liquid/vapour interface and when a bubble grows, particles slide on the bubble and settle around the base of the bubble at the crud/fluid interface. Basset and Thomas proposed to use the Asakura formalism for this phenomenon. The form of the deposit is different, so we can think that the mechanism must be different, but the driving factor is the vaporization rate as the Asakura mechanism. The constant $K_{trap}$ can be defined as the ratio of the volume of a particle skin around the bubble $V_{skin}$ to the volume evaporated $V_1$.

The boiling deposition rate by trapping [$kg.m^{-2}.s^{-1}$] is based on the Lister and Cussac model [17] and is expressed by:

$$\frac{dm}{dt} = K_{trap} \cdot \dot{m}_v \cdot \left( \frac{1+F_E}{2} \cdot C_0^{part} \right) \quad \textbf{(13)}$$

$$\text{with} \quad K_{trap} = \xi \cdot \int_0^t \frac{V_{skin}}{V_1} dt \quad \textbf{(14)}$$

and $\xi$ the proportion of particles trapped at the vapour/liquid interface, $V_{skin}$ the volume of the particle skin, $V_1$ the volume evaporated to form a bubble, $\dot{m}_v$ the vaporization rate [$kg.m^{-2}.s^{-1}$], $F_E$ the enrichment factor and $C_0^{part}$ the particle concentration in the bulk [$kg.kg^{-1}$], $\left( \frac{1+F_E}{2} \cdot C_0^{part} \right)$ is the average particle concentration around a bubble.

## 3.3 Erosion in boiling conditions

The erosion rate is higher in a two-phase flow than in a single-phase flow due to the turbulences generated by the bubbles collapsing close to the wall [17]. Furthermore, above a certain crud thickness, the deposit is eroded by spalling, thus releasing large particle agglomerates.
The erosion rate in boiling conditions [$kg.s^{-1}$] is expressed by:

$$\frac{dm}{dt} = \frac{E_{boil}}{\Psi} \cdot m_{erod} \quad \textbf{(15)}$$

with $E_{boil} = -\frac{\tau_{wall} \cdot \ln\left(1 - \frac{K_{boil}}{270}\right)}{75 \cdot \mu_{fluid}}$ the erosion coefficient [$s^{-1}$] (based on the Cleaver and Yates model [18]), $\tau_{wall}$ the shear stress at the wall [$kg.m^{-1}.s^{-2}$], $K_{boil}$ a constant in boiling conditions which is calibrated, $\mu_{fluid}$ the dynamic viscosity of the fluid [$kg.m^{-1}.s^{-1}$], $\Psi$ the resistance to erosion (Zakharov model [19]) and $m_{erod}$ the mass [kg] which can be eroded and which depends on a spalling thickness.

# 4 SIMULATIONS IN BOILING CONDITIONS USING THE OSCAR CODE

## 4.1 Comparative study of the mass transfer mechanisms in boiling conditions

In order to study the impact of each mechanism on crud growth in boiling conditions, we have carried out OSCAR simulations in PWR conditions with sub-cooled nucleate boiling by activating the growth mechanisms one after one. Note that the erosion mechanism and the single-phase mechanisms are always activated in this study.

The variations of the crud thickness as a function of time and of mechanisms are presented in Figure 8.

The crud thickness after a 350-day run reaches 8 µm without boiling. It is just above 10 µm due to the enrichment phenomenon. By just taking into account the deposition by vaporization, the thickness strongly increases and reaches almost 50 µm. The deposition by trapping has a low impact in PWR conditions; the thickness is just above 50 µm. With all mechanisms, the crud thickness reaches 70 µm, there is thus an amplifying effect with the enrichment factor.

In PWR sub-cooled nucleate boiling conditions, the major mass transfer mechanism is therefore the deposition by vaporization.

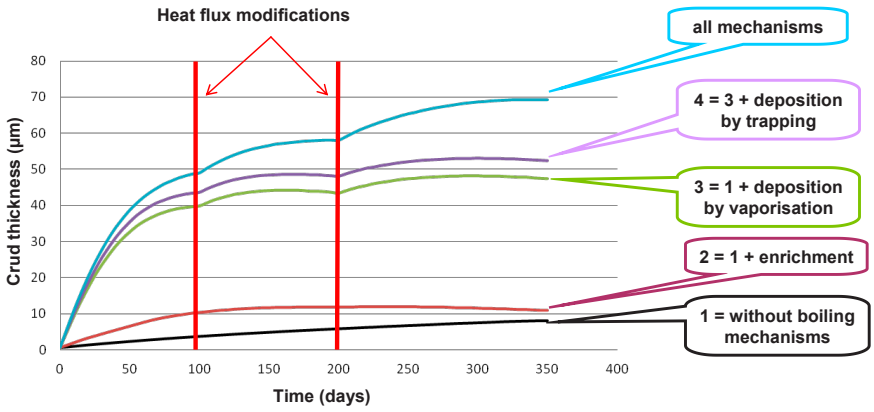


**Figure 8. Impact of each mechanism on the crud thickness in PWR conditions with sub-cooled nucleate boiling**

## 4.2 Simulation of a PWR case

The case is a 1300 MWe PWR (the description of the primary circuit is given in [2]). The first 4 operating cycles are simulated, the 2 first ones without boiling and the following ones with sub-cooled nucleate boiling. Boiling starts during cycle 3 and from the beginning of cycle 4. It is localized on the penultimate grid span (region C7 where the cladding temperature is the highest) of 1/3 of the fuel assemblies (Zone A of the core) which accounts for around 4% of the total fuel surface. The average heat flux density is 0.6 $MW.m^{-2}$; the temperatures and the power factor are given in Table 1. The PWR operates in Stretch-Out ("SO" in the figures below) at the end of cycle 4.

| Region C7 | Without boiling | With boiling |
|---|---|---|
| Bulk temperature (°C) | 323 | 325 |
| Wall temperature (°C) | 338 | 345 |
| Power factor | 1.08 | 1.2 |

**Table 1. PWR simulation – Temperatures and power factor of region C7 with and without boiling**

The crud thicknesses in regions C7A (with boiling) and C7B (without boiling) are presented in Figure 9. The maximum crud thickness is some µm without boiling, whereas it reaches 30 µm in sub-cooled boiling conditions. The crud is rich in Fe (and Ni) in boiling conditions, reflecting the fact that iron precipitates on the upper part of the fuel assemblies in boiling conditions (see Figure 10), whereas it is not the case in single-phase conditions. The crud thickness and composition are consistent with experimental data. Note that the deposit thickness is mainly determined by the vaporization rate (depending on the average heat flux density and the power factor) and by the erosion rate which is calibrated.

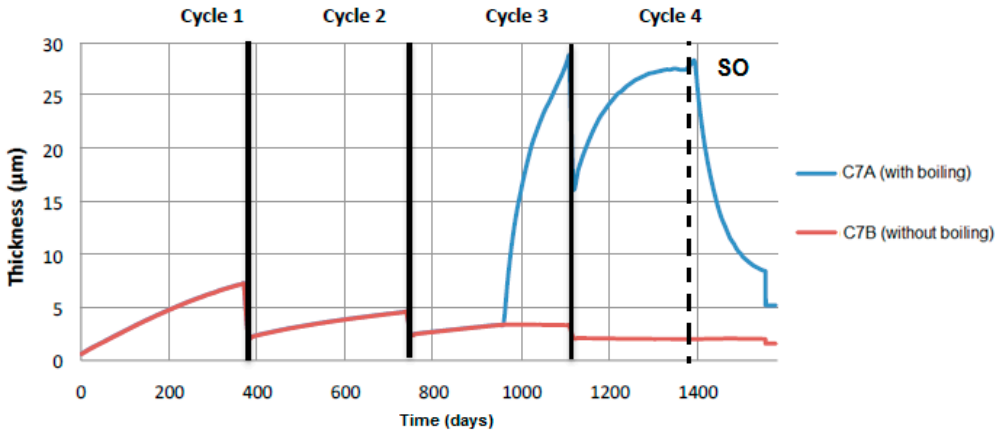


**Figure 9. PWR simulation - Crud thickness on grid span C7 with and without boiling**

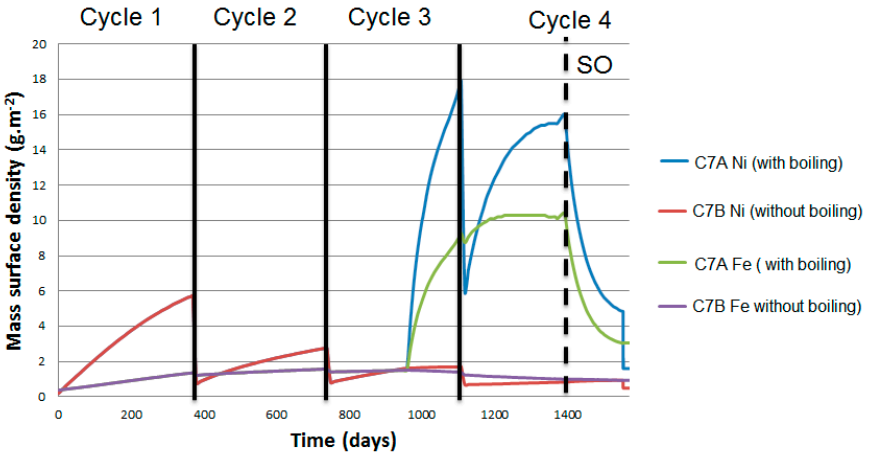


**Figure 10. PWR simulation – Composition of the crud on grid span C7 with and without boiling**

The erosion rate being higher in boiling conditions, the $^{58}$Co volume activity and, to a lesser extent, the $^{51}$Cr one increase a lot, up to 200-300 Bq.g$^{-1}$ in $^{58}$Co and 50-100 Bq.g$^{-1}$ in $^{51}$Cr (see Figure 11). The increase in $^{60}$Co and $^{54}$Mn is low. Due to the stretch-out, the volume activities tend to decrease because the boiling conditions are not met anymore.
These levels and variations are consistent with the experimental feedback (see Figure 1).

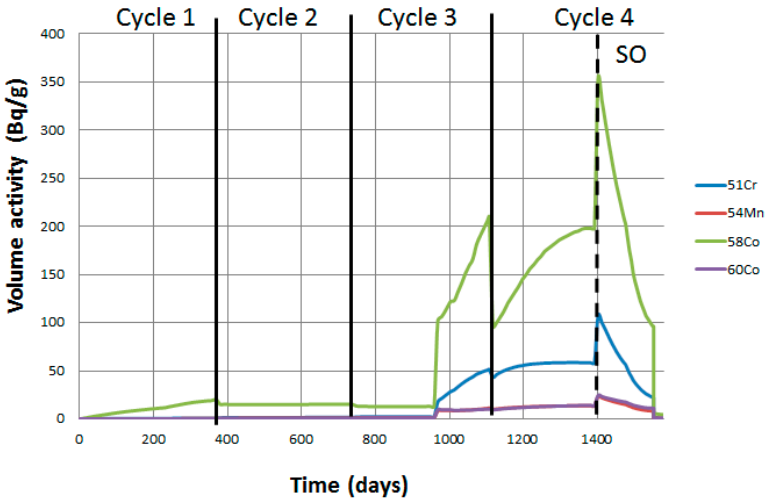


**Figure 11. PWR simulation – Volume activities of the primary coolant**

## 5 CONCLUSION

In order to reproduce volume activity increases observed during certain cycles in French PWRs, a modelling of the corrosion products transfer mechanisms in boiling conditions have been developed in the OSCAR code. Different phenomena have been modelled:

- Enrichment: concentration increases at crud-coolant interface,
- Boiling deposition by vaporisation: fluid vaporization at wall results in particle deposition and ion precipitation. As the crud growth, boiling occurs in the crud itself, so do the ion precipitation and deposition of the small particles. In PWR sub-cooled nucleate boiling conditions, this crud growth mechanism is the major one.
- Boiling deposition by trapping: some of the small particles trapped at the interface bubble/fluid make deposit when a bubble leaves the wall.
- Enhanced erosion: turbulences generated by bubbles collapsing close to the wall and spalling above a certain deposit thickness enhance erosion; it results in the release of particle agglomerates.

OSCAR simulations have shown that predicted crud thickness on fuel rods as well as volume activities in the primary coolant under nucleate boiling conditions are in good agreement with the field experience of French PWRs.

## REFERENCES

[1] EPRI, “PWR Axial Offset Anomaly (AOA) Guidelines“, TR 110070, Palo Alto, 1999.

[2] Dacquait F., Francescatto J., Broutin F., Génin J.B., Bénier G., You D., Ranchoux G., Bonnefon J., Bachet M., Riot G., “Simulations of corrosion product transfer with the OSCAR V1.2 code”, Nuclear Plant Chemistry Conference, Paris, 2012.

[3] Ferrer A., “Modélisation des mécanismes de formation sous ébullition locale des dépôts sur les gaines de combustible des Réacteurs à Eau sous Pression conduisant à des activités volumiques importantes », PhD thesis, Université de Strasbourg, 2013.

[4] Macbeth R.V., Tremberth R., and Wood R. W., “An investigation into effect of crud deposits on surface Temperature, dry-out and pressure drop, with forced convection boiling of water at 69 bar in an annular test section”, AEAW-R-705, 1971.

[5] Jones B.G., “Modeling and Thermal Performance Evaluation of Porous Crud Layers in Sub-Cooled Boiling Region of PWRs and Effects of Sub-Cooled Nucleate Boiling on

Anomalous Porous Crud Deposition on Fuel Pin Surface", Department Nuclear, Plasma and Radiological Engineering University of Illinois, 2005.

[6] Pan C., Jones B.G. and Machiels A.J., "Concentration level of solutes in porous deposits with chimneys under wick boiling conditions", University of Illinois, EPRI, 1987.

[7] March P., "Caractérisation et modélisation de l'environnement thermodynamique et chimique des gaines de combustible des réacteurs à eau sous pression en présence d'ébullition", PhD thesis, Université de Provence, 1999.

[8] Plancque G., You D., Blanchard E., Mertens V. and Lamouroux C., "Role of chemistry in the phenomena occurring in nuclear power plants circuits", Proceedings of the International Congress on Advances in Nuclear power Plants, ICAPP, 2-5 May 2011, Nice (France), 2011.

[9] Asakura Y., "Deposit of Iron Oxide on Heated Surfaces in Boiling Water", Hitachi Ltd., 1978.

[10] Unal H.C., "Maximum bubble diameter, maximum bubble-growth time and bubble-growth rate during the subcooled nucleate flow boiling of water up to 17.7 MN/m²", International Journal of Heat and Mass Transfer, 1976.

[11] Torigai K., Trans JSME, volume 32, pages 1263 1275, 1966.

[12] Charlesworth D. H., "Chemical Engineering Program Symposium Series", volume 6, 1970.

[13] Rassokhim N. G. *et al.*, "Iron oxide deposits on heat surfaces and their removal High Temperature and High Pressure Electrochemistry in Aqueous Solutions", 1976.

[14] Turner C. W., Liner Y. and Carver M. B., "Modelling magnetite particle deposition in nuclear steam generator and comparison with data plant", Atomic Energy Research Establishment, 1961.

[15] Basset M., Ardbeau N., McInernet J., Lister D. H., "Deposition of particles onto alloy-800 Steam Generator Tubes", Department of Chemical Engineering, University of New Brunswick, P. O. Box 4400, Fredericton, New Brunswick, Canada, E3B 5A3.

[16] Thomas D., Grigull U., "Experimental investigation of the deposition of suspended magnetite from the fluid flow in steam generating boiler tubes", Brennst-Warme-Kraft,1974

[17] Lister D. H. and Cussac F., "Modelling of particulate fouling on heat exchanger surfaces: influence of bubbles on iron oxide deposition", Heat Transfer Engineering, 2009.

[18] Cleaver J. W. and Yates B., "Mechanism of detachment of colloidal particles from a flat substrat in a turbulent flow", Journal of Colloid and Interface Science, 3, 1972.

[19] Zakharov B. M., Trofinov M. G., Guseva Y. I., Golovkin A. A. and Kononov V., "Bond strength of coating applied by the flame plating technique", Union Institute of Aviation Materials, 1970.